2018

Frost Growth Detection Using Capacitive Sensor

Yuchen Shen
University of Illinois at Urbana-Champaign, United States of America, yshen51@illinois.edu

Hongqing Jin
University of Illinois at Urbana-Champaign, United States of America, hj8@illinois.edu

Xiaofei Wang
University of illinois at urbana champaign, United States of America, wangxf@illinois.edu

Dynamic Frost Growth Detection Using Capacitive Sensor

Yuchen SHEN, Xiaofei WANG*

Department of Mechanical Science and Engineering,
University of Illinois at Urbana-Champaign,
Urbana, IL, USA
E-mail: wangxf@illinois.edu

* Corresponding Author

ABSTRACT

In this work, the frost growth was detected using capacitive sensing approach. An interdigital electrode was designed and fabricated based on the fringing effect. Frost growth under different wall temperature, air temperature was conducted and also observed using high speed camera. The results show that the reading of the capacitive sensing can represent the frost thickness in a resolution of 0.00069mm- 0.0013 mm depending on different frost property. The capacitive sensing can follow the frost thickness changing trend very well and the capacitance changing rate can reflect different frost growth stage. The frost thickness is higher in a lower wall surface temperature, and the effect of air temperature on the frost thickness is depending on the frost growth stage. This work has a great potential for understanding the frost growth mechanism and defrost control.

1. INTRODUCTION

Frost buildup on surfaces could be an undesired situation in many applications (Guo *et al*., 2008; Zhi *et al*., 2015; Da Silva *et al*., 2017; Hwang and Cho, 2014; Zhang *et al*., 2018; Jia *et al*., 2018). In refrigeration and heat pump system, typically, frost grows on the fin surface of the heat exchanger due to different environmental/operational conditions. On one hand, it can block the air flow and increase air-side pressure drop; on the other hand, it can increase the thermal resistance and deteriorate heat transfer performance. As a result, frost buildup can significantly reduce the system's COP. It is very common that systems encountered frost buildup have to run the defrost cycle, which relies on either the pre-build models or real time detection or both.

The frost growth is a complex dynamic process and usually characterized by the frost parameters, of which the frost thickness and density (porosity) are important parameters. The frost thickness and density (porosity) vary under different working conditions, including different surrounding air humidity, temperature, different air flow rate, different wall temperature, surface wettability, *et. al.*; they also vary with time as the frost layer builds up, because the frost/air interface temperature and local air humidity keep changing with time due to the variation of the thermal conductivity along the frost layer. There are a lot of modeling work to predict frost growth (Hermes *et al*., 2009; Kim *et al*., 2008; Yang *et al*, 2006), and most models have one or several parameters heavily relying on experimental measurement, even for pure numerical work, they usually start with some initial assumptions and verify later with experimental results. Therefore, dynamically detecting frost growth is very important for both effective defrost control and precise frost modelling.

There are a lot of approaches to detect frost growth. CCD images and image processing is the most commonly used method (Lee and Lee, 2018; Liu and Kulacki, 2018; Kim *et al*., 2015; Wu *et al*., 2016), which provides numerous information for understanding frost growth and could precisely measure frost thickness given a high resolution CCD selected for the observation. However, it is difficult to give a complete spatial detection along the surface due to the position of camera and light source, for the same reason, some measurement might be intrusive to air flow. And it is also challenging for measurement in limited space or poor light source in real application. Other methods have been

proposed as well. Ostin and Andersson (1991) measured the frost growth under forced airflow using micrometer with a resolution of 0.005mm, in which the micrometer they used must touch the frost and the device might affect the airflow over the surface and induced errors. Qu *et al*. (2006) measured the frost thickness variation using a laser displacement gauge with an uncertainty of 0.01mm. Query (1989) reported a fiber optic sensor that could be used to detecting accumulated frost by sensing the light transmission amount on cold surface. Although these frost detection methods provide a high accuracy measurement, they are still far from the practical applications for defrost control, due to the large device cost and strict space requirement. Capacitive sensing method can be compact, effective and flexible, especially in limited space or extreme environment. The built-in interdigital electrodes (IDEs) for capacitive sensing can be very sensitive with a high resolution and its performance can be optimized by its geometry and substrate design (Igreja *et al*., 2004), which has been adopted in a lot of applications, such as real-time ice detection (Zhi *et al*., 2015), water level measurement (Chetpattananondh *et al*., 2014) chemical sensor (Kitsara *et al*., 2007; Abu-Abed *et al*., 2008), humidity sensor (Fürjes *et al*., 2003), food inspection (Mohd Syaifudin *et al*., 2012). However, frost, as a mixture of ice and air, has a very low dielectric constant of about 1~53 depending on frost porosity. The frost thickness, porosity and interfacial morphology vary both spatially and temporally under different conditions, which makes the detection of frost using capacitance sensing much more difficult compared with detections of object with constant properties or high dielectric constant.

In this work, a pair of gold deposited IDEs is designed to capture frost growth under different conditions. CCD imaging is also used to quantify frost thickness for calibration and comparison. The capacitance sensor can measure frost thickness with high sensitivity and precisely reflect the variation of frost properties during different frost growth stage. This work has a great potential in defrost control and important for frost mechanism understanding.

2. EXPERIMENTAL APPARATUS AND PROCEDURE

2.1 Experimental setup

The experiments were conducted in a wind tunnel, as shown in Figure 1, in which the environmental condition (the air temperature, velocity and relative humidity) can be controlled at a desired value. The air temperature is controlled by a cooling coil connected to an isothermal bath and a heater as well, within a range of ~5°C to ~ 45°C. The maximum air velocity is about 12.0 m/s and can be adjusted by the blower speed. The relative humidity is controlled by a humidifier located in the front of the blower, with an uncertainty of ± 5%. The air under the desired condition flows through the mixer, honey comb and contraction area in the wind tunnel and get the temperature distribution measured, and then it passes the test section labeled as 9 in Figure 1, with the temperature, pressure drop and velocity measured, and flows back to the starting section.

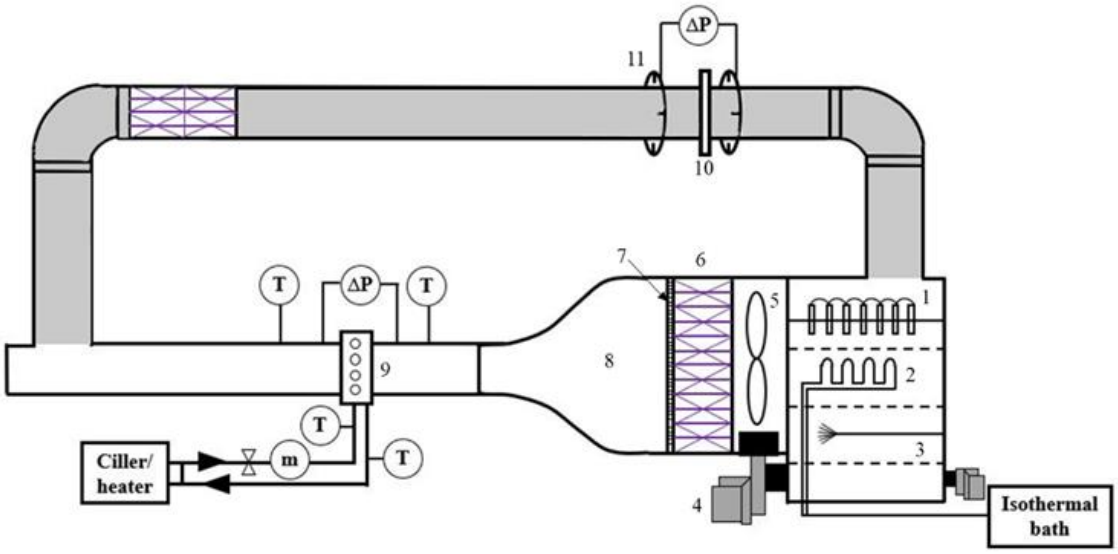

Fig 1: Schematic diagram of experiment setup: 1. heater; 2. cooling coil; 3. cold mist humidifier; 4. blower; 5. mixer; 6. honey comb; 7. screen; 8. contraction; 9. test section; 10. orifice plate; 11. D & D/2 pressure taps

Frost grows on the aluminum surface of a cold plate which is located in 9 in Figure 1. The surface temperature is controlled to a range of -20°C to ~ 30°C through a chiller/heater connected to it. 4 thermocouples were embedded in channels below the surface with a distance to the surface of 2.5 mm, to measure the surface temperature of the cold plate. The capacitance sensor is located on one side of the cold plate and the CCD camera is on the other side, as shown in Figure 2. The dynamics of the frost growth is captured by the CCD camera with a sample rate of 24 fps. The frost thickness can be then measured based on image processing programmed in Matlab2012.

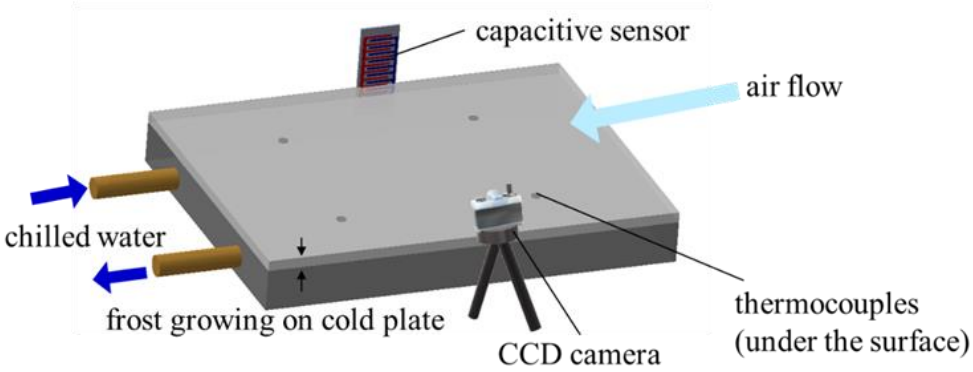

Fig 2: Test section setup

2.2 Capacitance sensor- the principle and fabrication

The capacitance sensor, shown in Figure 3, includes an analog-to-digital converter, a PCB connector, and the electrodes. The analog-to-digital converter (FDC2214 from Texas Instruments) can simultaneously convert analog signals for 4 channels with a resolution of 0.0001pF and sample rate of 40 to 80Hz depending on the environmental noise. The PCB connector is fabricated with the designed electrical circuit to connect the electrodes to the digital converter, which has the converter input connected on one surface and the electrodes output attached on the other surface. The printed electric conducting wire connects them through the two surfaces of the connector.

The electrodes (interdigital electrodes) are the core part for sensing the capacitance changing during the frost growth, which includes 3 layers, as shown in Figure 4. A thin layer of gold (0.5μm in thickness) was deposited on the silicon wafer substrate by metal lift-off method in a pair of comb pattern, as shown in Figure 5. On the top of the electrodes layer, 1μm SiO_2 was deposited by chemical vapor deposition approach for protection and insulation.

The comb pattern of the electrodes has finger width (f) of 150μm, gaps distance (g) of 50μm, and total height of 15 mm, which makes the total metallization ratio $\eta=f/(f+g)$ of 75%, and effective measuring height for the target of 15 mm. The electrical potential of the pair electrodes is at a fixed value ((+V or 0 respectively), and the capacitance reading changes from the initial value with air to a different value as the target appears close by due to the fringing effect. The variation of the capacitance reading is related to the target height, the target dielectric constant for a fixed structure electrodes. And the resolution of the sensor used in this work for frost thickness is 0.000694mm/0.001pF ~ 0.0013mm/0.001pF depending on the frost porosity.

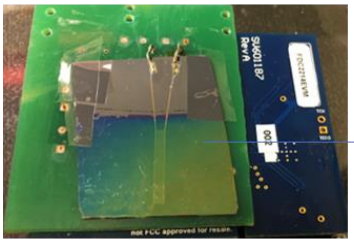

Figure 3. packaged capacitive sensor with electrodes

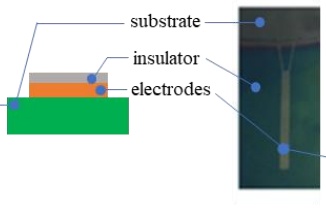

Figure 4. schematic view of the electrode of capacitive frost sensor

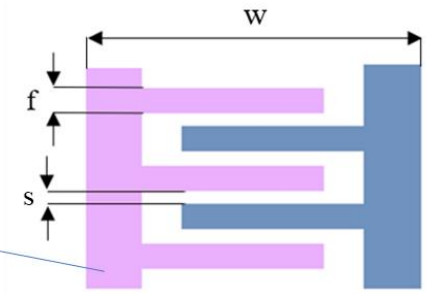

Figure 5. layout of interdigital electrodes

2.3 Uncertainty and test matrix of the experiment

The uncertainty and range in the reading of all measured parameters are listed in Table 1.

Table 1: Range and uncertainty of the measured parameters

Measured parameters/unit	Range	uncertainty
Temperature/°C	-60℃ - 100℃	±0.1
Air velocity/ ms^{-1}	0 - 12m/s	±0.0073% of full scale
Relative humidity	30% - 95%	±1%
Pressure drop	0 - 5 in. W.C.	±0.14% of full scale
Capacitance	0 - 250nF	±0.001
Frost thickness/mm	0 - 8mm	±0.014mm

The frost growth on flat aluminum surface was observed under different conditions, including air velocity, air temperature and flat surface temperature, both images and capacitance reading from the sensor are captured and the test matrix is shown in Table 2.

Table 2: Test matrix

Run	T_w (℃)	T_a(℃)	u_a (m/s)	RH(%)
1	-8.0	11.5	2.943	55
2	-5.6	11.3	2.987	57
3	-3.0	11.6	3.010	57
4	-7.9	13.5	2.977	56
5	-8.0	16.1	3.033	55

3. RESULTS AND DISCUSSION

3.1 Frost growth under different surface temperature

The measured frost thickness (δ, dash line), capacitance reading (C, solid line) under different wall temperature (-8.0 ℃, -5.5℃ & -3.0 ℃) is shown in Figure 6. Air was controlled at the constant temperature (11.3℃), relative humidity (54% ~ 57%), and velocity (3.0 m/s). Around 220 minutes of frost growth was recorded, and it is divided into 4 different timing slots as shown in (a)-(d) in Figure 6. It can be found that the frost thickness increases with time as frost growing, from 0 at the beginning to around 2mm at the end of the observation. The frost thickness is larger at a low cold surface temperature compared with that at a high cold wall temperature, which has been well demonstrated after 15 minutes of the frost growth. The capacitance reading is well tracing the frost thickness changing with time, as well as its changing with cold wall temperature, which keeps increasing with time as frost growing, and is larger at the lower wall temperature. The range of capacitance changing during the whole frost growth period is around 1.500 pf, 2.200 pf, and 2.500 pf for surface temperature of -3.0℃, -5.5 ℃ and -8.0 ℃, respectively, which can provide enough sensitivity to detect detailed frost growth given a resolution of 0.001pf for the capacitance reading.

The frost thickness measured by image processing keeps slowly increasing with time at a relative constant rate during the whole recorded frost growth period except for a turn around 6-12 minutes from the beginning under different surface temperature, as shown in Figure 6 (a). However, the capacitance reading from the sensor has the increasing rate fluctuated with time. Take the capacitance reading of frost growth at the surface temperature of -8.0 ℃as an example, the capacitance reading increases in a different rate with time, at the beginning (0-3 minutes) in a very small rate, and then a big rate (around 3-9 minutes), after that the increasing rate drops down again (9-22 minutes roughly). The increasing is in a higher rate again from around 22-37 minutes, and it turns afterwards at around 55 minutes, 72 minutes, 77 minute, 90 minutes and so on. Referring to the surface images, it can be found that the fluctuation of the capacitance increasing rate reflects the condensation, solidification, crystal growth, melting on the frost-air interface and maturing growth, as shown in Figure 7(a), droplets coalesce at 4.326min, 8.123min and 8.832min, then solidification happens at 6.734min, 10.232min and 10.453min for T_w = -8℃, T_w = -5.5℃ and T_w = -3℃, respectively, which is close to the prediction by capacitance reading. The second fast increase in capacitance reading appears at 32.5min, 54.8min and 47.5min for T_w = -8℃, T_w = -5.5℃ and T_w = -3℃, respectively, and images in Figure 7(b) show that large crystal branches melt down between 34.142~36.324min;

57.634~60.432min and 47.754~48.242min, correspondingly. Meanwhile, frost density increases, since the melting water from crystals diffuses in the porous space of frost structure, and the frost thermal conductivity increases as well. This combined effect causes the fluctuation of capacitance reading during the crystals growth period. Though some crystal branches fall down, newly formed branches keep sticking out, this dynamic process can be expressed in capacitance reading as a steady but gradually slow down increase, since the crystals have the tendency to melt as the frost surface temperature increasing, and the frost growth rate is also slowing down. The last changing rate peak happens at 85.3min and 91.7min for T_w = -5.5℃ and T_w = -3℃, respectively, as shown in Figure 6(c). For wall temperature at -8.0℃, there are two peaks observed, at 73.2min and 95.2min. Frost images in Figure 2(c) show that frost surface roughness is much smaller than early growth period, and less crystal branches can be recognized, at 89.323min, 92.531min and 98.243min for T_w = -8, T_w = -5.5℃ and T_w = -3℃, as Figure 7(c) shows. The last peak in capacitance increasing rate can be explained by the condensed water vapor staying on the frost surface instead of forming a crystal branch, due to the high frost surface temperature. After that, all condensed water drains to the base and forms an ice layer. Frost thickness further increase can be viewed as the developing of ice layer, which forms a new dynamic equilibrium. No fluctuation in capacitance reading was noticed in this mature growth period, as Figure 6(d) shows.

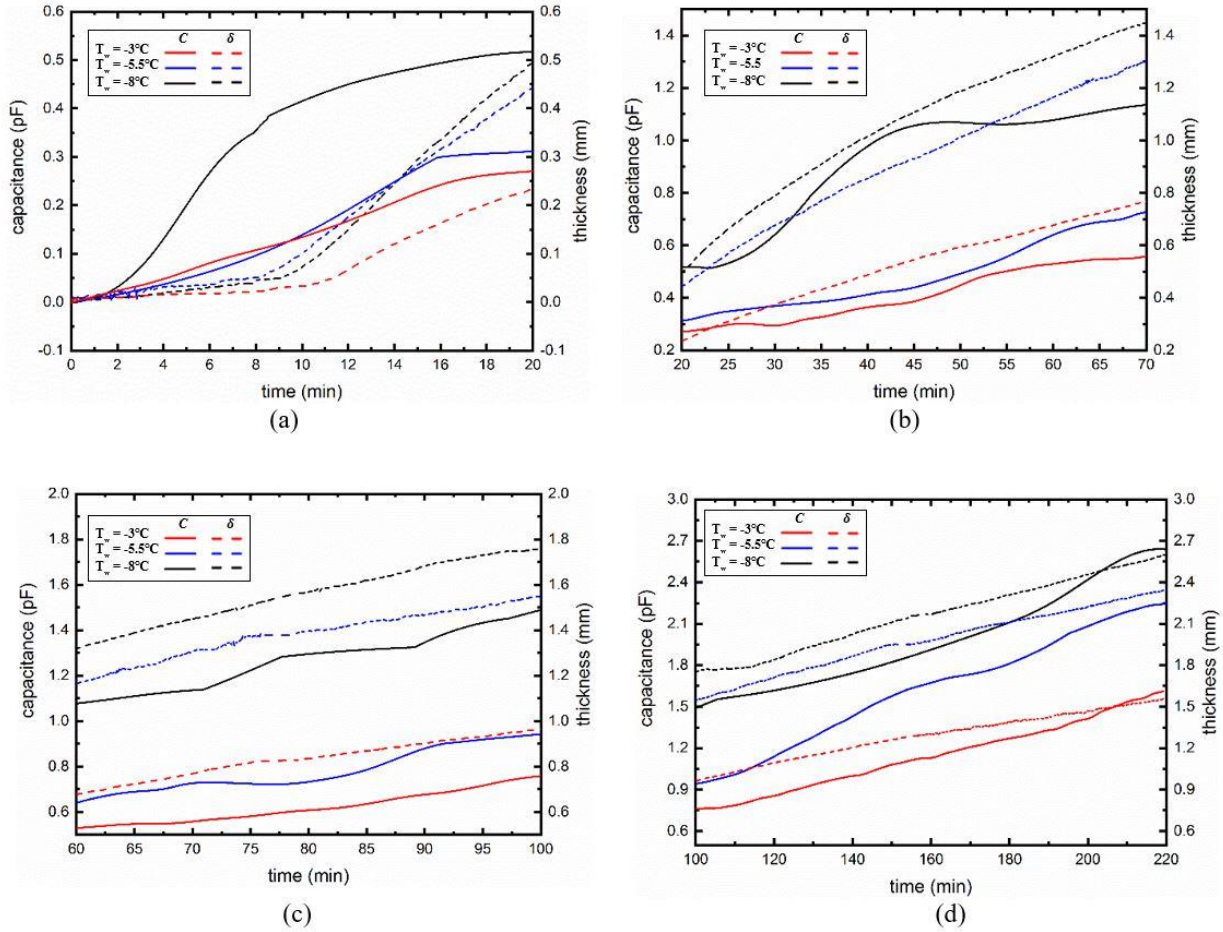

Fig 6: The frost thickness and the capacitance reading at wall temperature of -8.0℃, -5.5℃ and -3.0℃ within 220min growth.

3.2 Frost growth at different Air temperature

Figure 8 shows frost growth at T_a = 11.3℃, T_a = 13.5℃ and T_a = 16.0℃, while other parameters, wall temperature (-8.0℃), relative humidity (55%~57%) and air velocity (3m/s) were kept the same. It can be noted that three stages of frost growth, droplets condensation/solidification, crystals growth /melting and frost mature growth, are represented as the capacitance changing rate. By comparing the time of these changing, it indicates that the frost mature growth starts at 25min at T_a = 16℃, while for T_a = 13.5℃ and T_a = 11.3℃, mature growth happens at 50min

and 72.5min, respectively. When increasing the airside temperature, however, frost thickness growth varies with time. Within 110min after condensation starts, frost at T_a = 16℃ grows thickest among three cases. It can be explained by airside vapor concentration gradient in different airside temperature. When the airside temperature arises, the humidity ratio must increase to keep the same relative humidity, which leads to a higher airside vapor concentration, so does the driving force of vapor diffusion. Therefore, more frost tends to form in higher airside temperature condition. Meanwhile, increasing in airside temperature also results in melting of crystals, as frost thickness increasing, growth rate will decrease, which explains that eventually at 220min, thickest frost layer formed at T_a =11.3℃ case.

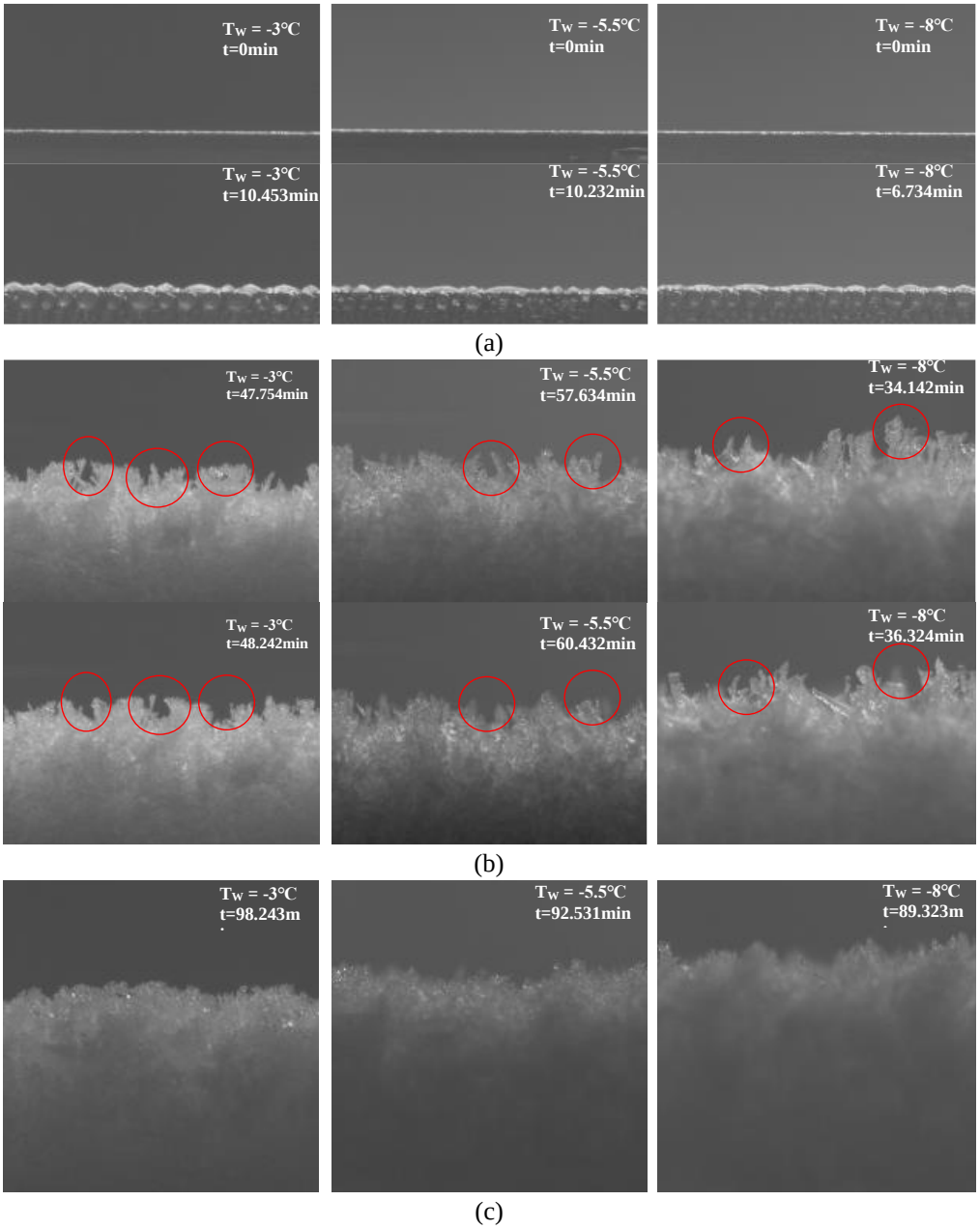

Fig 7: CCD images of frost formation at T_w = -8.0℃, T_w = -5.5℃ and T_w = -3.0℃. (a) the droplets condensation – solidification; (b) the crystals melting down; (c) frost mature growth.

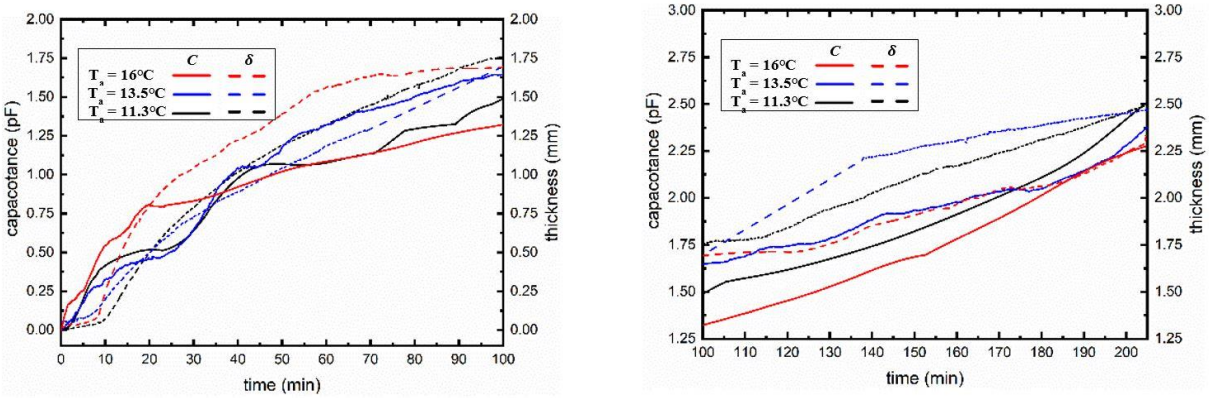

Fig 8: The frost thickness, capacitance reading at air temperature of 11.3℃, 13.5℃ and 16℃

4. CONCLUSIONS

A real-time frost growth detection was conducted using capacitive sensing approach in this work. An interdigital electrode was designed and fabricated based on the fringing effect. The frost growth was also observed using high speed CCD and image processing to measure the frost thickness for comparison. Effect of different cold surface temperature, air temperature on frost growth were compared and discussed based on both approach. The results show that:

The capacitive sensing measurement for the frost thickness can reach to a resolution of 0.00069mm- 0.0013 (depending on the frost porosity).

Both the capacitive sensing approach and the image processing observes the frost thickness increasing with time, however, the capacitive sensing can reflect the frost growth variation during different growth stage and provide more information of frost growth.

The frost thickness is higher in a lower wall surface temperature, and the effect of air temperature on the frost thickness is depending on the frost growth stage, it takes a shorter time for the frost to reach the mature growth stage under a high air temperature compared that under the low air temperature.

REFERENCES

Abu-Abed, A. S., & Lindquist, R. G. (2008). Capacitive interdigital sensor with inhomogeneous nematic liquid crystal film. *Prog. Electromagn. Res., 7*, 75-87.

Amini, M., Pishevar, A. R., & Yaghoubi, M. (2014). Experimental study of frost formation on a fin-and-tube heat exchanger by natural convection. *Int. J. Refrig., 46*, 37-49.

Aragones, J. L., MacDowell, L. G., & Vega, C. (2010). Dielectric constant of ices and water: a lesson about water interactions. J. Phys. Chem. A, 115(23), 5745-5758.

Byun, J. S., Jeon, C. D., Jung, J. H., & Lee, J. (2006). The application of photo-coupler for frost detecting in an air-source heat pump. *Int. J. Refrig., 29*(2), 191-198.

Chetpattananondh, K., Tapoanoi, T., Phukpattaranont, P., & Jindapetch, N. (2014). A self-calibration water level measurement using an interdigital capacitive sensor. *Sens. Actuator A-Phys., 209*, 175-182.

da Silva, D. L., Melo, C., & Hermes, C. J. (2017). Effect of frost morphology on the thermal-hydraulic performance of fan-supplied tube-fin evaporators. *Appl. Therm. Eng., 111*, 1060-1068.

Fürjes, P., Kovács, A., Dücso, C., Ádám, M., Müller, B., & Mescheder, U. (2003). Porous silicon-based humidity sensor with interdigital electrodes and internal heaters. Sens. Actuator B-Chem., 95(1-3), 140-144.

Guo, X. M., Chen, Y. G., Wang, W. H., & Chen, C. Z. (2008). Experimental study on frost growth and dynamic performance of air source heat pump system. *Appl. Therm. Eng., 28*(17-18), 2267-2278.

Hayashi, Y., Aoki, A., Adachi, S., & Hori, K. (1977). Study of frost properties correlating with frost formation types. J. Heat Transfer, 99(2), 239-245.

Hermes, C. J., Piucco, R. O., Barbosa Jr, J. R., & Melo, C. (2009). A study of frost growth and densification on flat surfaces. *Exp. Therm. Fluid. Sci., 33*(2), 371-379.

Hwang, J., & Cho, K. (2014). Numerical prediction of frost properties and performance of fin–tube heat exchanger with plain fin under frosting. Int. J. Refrig., 46, 59-68.

Igreja, R., & Dias, C. J. (2004). Analytical evaluation of the interdigital electrodes capacitance for a multi-layered structure. Sens. Actuator A-Phys., 112(2-3), 291-301.

Jia, Y., Xu, X., Li, Y., Liang, X., & Yao, M. (2018). Experimental studies on frost and defrost of fine tube bundles under coolant temperature between− 20 and− 58° C. Int. J. Heat Mass Transfer, 116, 617-620.

Kim, D., Kim, C., & Lee, K. S. (2015). Frosting model for predicting macroscopic and local frost behaviors on a cold plate. Int. J. Heat Mass Transfer, 82, 135-142.

Kim, J. S., Yang, D. K., & Lee, K. S. (2008). Dimensionless correlations of frost properties on a cold cylinder surface. *Int. J. Heat Mass Transfer, 51*(15-16), 3946-3952.

Kitsara, M., Goustouridis, D., Chatzandroulis, S., Chatzichristidi, M., Raptis, I., Ganetsos, T., ... & Dias, C. J. (2007). Single chip interdigitated electrode capacitive chemical sensor arrays. Sens. Actuator B-Chem., 127(1), 186-192.

Lee, J., & Lee, K. S. (2018). The behavior of frost layer growth under conditions favorable for desublimation. Int. J. Heat Mass Transfer, 120, 259-266.

Lee, Y. B., & Ro, S. T. (2005). Analysis of the frost growth on a flat plate by simple models of saturation and supersaturation. *Exp. Therm. Fluid. Sci., 29*(6), 685-696.

Liu, Y., & Kulacki, F. A. (2018). An experimental study of defrost on treated surfaces: Effect of frost slumping. *Int. J. Heat Mass Transfer, 119*, 880-890.

Mohd Syaifudin, A. R., Mukhopadhyay, S. C., & Yu, P. L. (2012). Modelling and fabrication of optimum structure of novel interdigital sensors for food inspection. Int. J. Numer. Model Electron Network Dev. Field, 25(1), 64-81.

Nassr, A. A., Ahmed, W. H., & El-Dakhakhni, W. W. (2008). Coplanar capacitance sensors for detecting water intrusion in composite structures. Meas. Sci. Technol., 19(7), 075702.

Östin, R., & Andersson, S. (1991). Frost growth parameters in a forced air stream *Int. J. Heat Mass Transfer, 34*(4-5), 1009-1017.

Qu, K., Komori, S., & Jiang, Y. (2006). Local variation of frost layer thickness and morphology. Int. J. Therm. Sci., 45(2), 116-123.

Query, D. S. (1989). U.S. Patent No. 4,860,551. Washington, DC: U.S. Patent and Trademark Office.

Wu, X., Hu, S., & Chu, F. (2016). Experimental study of frost formation on cold surfaces with various fin layouts. *Appl. Therm. Eng.*, 95, 95-105.

Yang, D. K., Lee, K. S., & Cha, D. J. (2006). Frost formation on a cold surface under turbulent flow. *Int. J. Refrig., 29*(2), 164-169.

Zhang, L., Jiang, Y., Dong, J., Yao, Y., & Deng, S. (2018). An experimental study of frost distribution and growth on finned tube heat exchangers used in air source heat pump units. *Appl. Therm. Eng., 132*, 38-51.

Zhi, X., Cho, H. C., Wang, B., Ahn, C. H., Moon, H. S., & Go, J. S. (2015). Development of a Capacitive Ice Sensor to Measure Ice Growth in Real Time. *Sensors*, *15*(3), 6688-6698.

ACKNOWLEDGEMENT

This work received financial support from the Air Conditioning and Refrigeration Center (ACRC) at the University of Illinois at Urbana-Champaign.